

***In situ* Growth of Gold Nanoparticles Based on Simultaneous Green Reduction by Methylene Blue for Non-Enzymatic Glucose Sensing**

Wenyuan Zhu¹, Xiaoya Li¹, Weihong Liu¹, Zuodong Chen¹, Jianping Li¹ and Hongcheng Pan^{1,2,3,*}

¹ College of Chemistry and Bioengineering, Guilin University of Technology, 12 Jiangan Road, Guilin 541004, P. R. China.

² Guangxi Colleges and Universities Key Laboratory of Food Safety and Detection, Guilin University of Technology, 12 Jiangan Road, Guilin 541004, P. R. China.

³ Guangxi Key Laboratory of Electrochemistry and Magnetochemistry Functional Materials, Guilin University of Technology, 12 Jiangan Road, Guilin 541004, P. R. China.

*E-mail: hepan@163.com

Received: 23 February 2017 / Accepted: 5 April 2017 / Published: 12 May 2017

We presents a novel approach for *in situ* growth of highly-dispersed gold nanoparticles (AuNPs) on the electropolymerized methylene blue (PMB)/ITO electrode (Au/PMB/ITO) without using additional binding molecules and toxic reductants. Methylene blue (MB) monomers remaining in the PMB films on ITO served as both the reductant to form AuNPs by reducing AuCl⁴⁻, and as anchoring sites for *in situ* growth of AuNPs via the electrostatic interaction between AuCl⁴⁻ and positively charged MB that avoids the aggregation of AuNPs, thereby improving their dispersity. Cyclic voltammetry (CV), differential pulse voltammetry (DPV), scanning electron microscope (SEM), UV–Vis spectroscopy (UV–Vis) and Fourier transformation infrared spectroscopy (FTIR) were used to characterize the resulting polymer and nanoparticles. The as-prepared Au/PMB/ITO exhibited an excellent electrocatalytic activity towards glucose oxidation with a high sensitivity of 312 $\mu\text{A mM}^{-1} \text{cm}^{-2}$ at a low operating potential of 0.04 V.

Keywords: Gold Nanoparticles; In Situ Growth; Methylene blue; non-enzymatic glucose sensing

1. INTRODUCTION

Due to attractive properties such as large specific surface area, good electrical properties and high electrocatalytic activity, gold nanoparticles (AuNPs) are widely used in electrode modification by improving the analytical sensitivity and selectivity[1-3]. To date, there are numerous approaches to attach AuNPs onto the surface of electrodes, such as electrochemical deposition, chemical reduction,

and seed-mediated growth method, depending on the materials and the substrates[4-10]. Electrochemical deposition is an easy and rapid alternative method to prepare AuNPs, but the amount and size of AuNPs are difficult to control. Although the latter two methods are popular, reducing agents used such as NaBH_4 and N_2H_4 are highly toxic[11]. Therefore, considerable efforts has been devoted to explore new and green reductants to prepare AuNPs, instead of NaBH_4 and N_2H_4 .

Methylene blue (MB) is a water-soluble nontoxic organic dye with two tertiary amine groups at phenothiazine skeleton and highly conjugated structure[12]. Behaving as an electron actuator, MB displays a fast and reversible redox reaction[9]. Due to excellent catalytic and photoelectrochemical properties, the polymeric films of MB have practical uses in many applications and can be obtained by different techniques[14-16]. Among these, electropolymerization is the most useful technique to obtain polymer films[17]. Hichem, Schlereth and co-workers have comprehensively investigated the electropolymerization film and found that it might be not homogeneous but still contained remaining traces of MB monomer, which resulted in their particular properties[18, 19].

In the present work, we described a new approach for in situ growth of highly-dispersed AuNPs on PMB/ITO electrode(Au/PMB/ITO) without using additional binding molecules and toxic reductants, in which MB monomer remaining in the PMB film on ITO served as not only the reductant to form AuNPs by reducing AuCl_4^- into Au^0 , but also as anchoring sites for AuNPs in situ growth via the electrostatic interactions between positively charged MB and AuCl_4^- to prevent the aggregation of AuNPs, thereby improving their dispersity. The as-prepared Au/PMB/ITO exhibited a very high activity toward the electrooxidation of glucose at a low operating potential.

2. EXPERIMENTAL

2.1. Chemicals and materials

Methylene blue, ethylene glycol, sodium acetate, sodium chloride, acetone and anhydrous ethanol were purchased from Shanghai Biochemical Reagent Company (China). ITO-coated glass (resistance: $30\text{-}60\ \Omega/\text{cm}^2$) were purchased from Kaivo Optoelectronic (Zhuhai, China). All chemicals were used of analytical grade and all solutions were prepared with twice-distilled deionized water.

2.2. Electropolymerization of MB on ITO

A sheet of ITO ($3\text{cm}\times 1.3\text{cm}$) was sonicated with acetone, anhydrous ethanol and twice-distilled deionized water for about 5min, respectively. The PMB/ITO electrode was prepared according to the process described by Ma et al. [15]. Briefly, the ITO substrate was immersed in 0.2 M phosphate buffer solution (pH 7.0) containing 2.0 mM MB monomer, by cycling electrodes between -0.6 and +1.4 V vs Ag/AgCl for 40 cycles at a scan rate of 100 mV/s. After rinsed thoroughly with twice-distilled water to remove any residual growing media, the resulting PMB/ITO was stored at 4 °C for use.

2.3. In situ growth of AuNPs on PMB/ITO

In situ growth of AuNPs could be carried out in a bath (37°C) for desired time by immersing PMB/ITO substrate into a 10ml growth solution containing 300 μL PBS (0.2 M pH = 6.0), 2 mL distilled water, 80 μL 1% HAuCl_4 and 50 μL cetyltrimethylammonium chloride (CTAC).

2.4. Characterization and electrochemical measurements

All electrochemical experiments in this research were performed using electrochemical workstation (Mode CHI660B, Chenhua Co. Ltd., Shanghai) with a conventional three-electrode system consisting of the bare or modified ITO electrode as working electrode, Ag/AgCl as a reference electrode, and a platinum wire as an auxiliary electrode. FTIR spectra were obtained on a Bruker Vector 22 spectrophotometer (Bruker, Germany) using KBr pressed disks. UV-vis absorption spectra were recorded on a CARY 50 spectrophotometer (Varian, USA). SEM images were obtained using a JEOL JSM2010F instrument.

3. RESULTS AND DISCUSSION

3.1. Electropolymerization of MB on ITO substrate

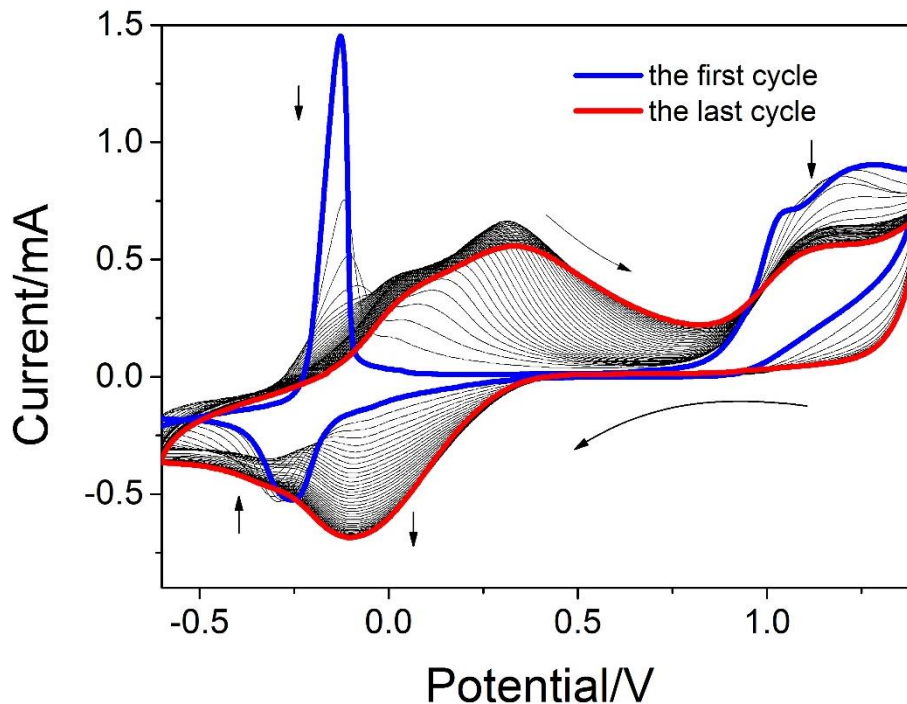


Figure 1. cyclic voltammogram of electropolymerization of methylene blue (solution: 0.2 M pH7.0 PBS, 2.0 mM MB, scan rate: 100 mV/s)

Fig.1 shows the cyclic voltammogram obtained during film growth. The first cycle of this voltammogram (blue curve) shows an initial reversible redox couple situated at -80 mV and -280 mV attributed to the oxidation and reduction of MB monomer, respectively, and another oxidation peak at ca. 1100 mV resulting from the formation of radical cation. During cycling, the peaks decrease in intensity and a novel redox wave couple appears at ca. 320 mV (oxidation) and -120 mV (reduction) corresponding to the polymer increase with successive cycles, which takes a maximum after about 40 cycles. The last cycle of this voltammogram (red curve) indicates that polymer film is not homogeneous but still contains few remaining traces of MB monomer, which is in accordance with those obtained by Hichem et al.[19].

Absorption spectra recorded with UV–visible spectrophotometer shown in Fig.2, show similarity for electropolymerized PMB and MB monomer except the fact that a novel wave appears at ca. 680 nm attributed to the polymer. This fact confirms polymerization process and is in accordance with the CV results above.

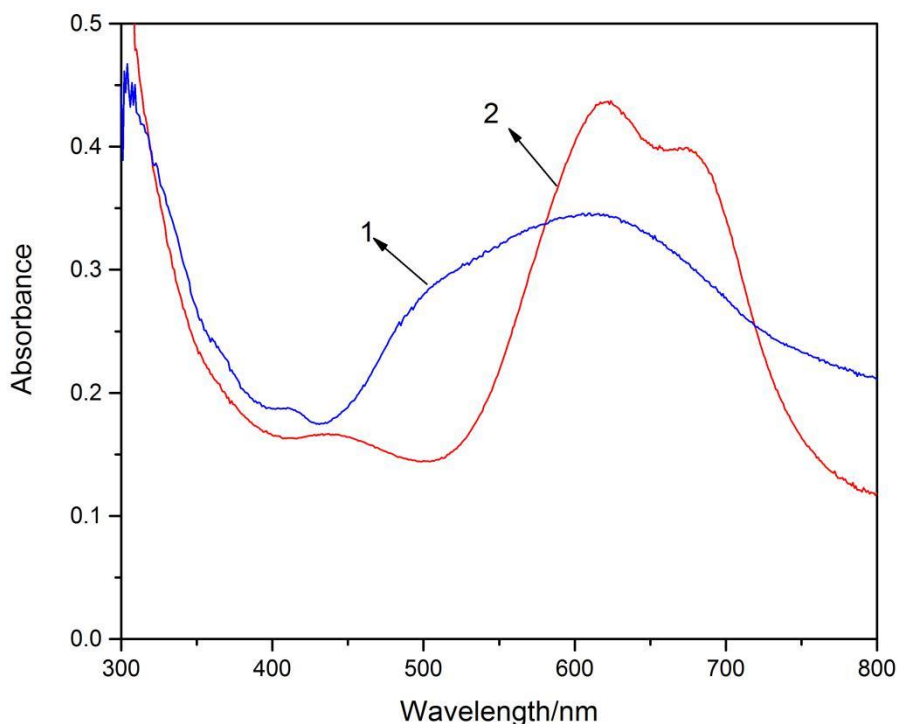


Figure 2. UV–vis spectra of coated MB monomer (1) and electropolymerized PMB (2) on the ITO electrodes.

FTIR spectroscopy was conducted to investigate the different structures of electropolymerized PMB and MB monomer shown in Fig.3. These spectra are almost similar to the spectra obtained in previous works [19, 20]. Two sharp peaks are seen in both spectra for phenyl ring stretching (C-C) at 1615 cm^{-1} and asymmetric C-N stretching at 1400 cm^{-1} except that the peak shape is sharp in the PMB spectrum (Fig. 3a). There are some differences between the two FTIR spectra: The peak at 1367 cm^{-1} becomes intensive in PMB spectrum (Fig. 3a), which is attributed to alkyl C-N stretching mode [19].

The peak at 1045 cm^{-1} associated with C-H vibration in MB spectrum (Fig. 3b) almost disappears in PMB spectrum. All results suggest that a linkage between the carbon atom of phenothiazine ring and the nitrogen atom of tertiary amine is a possible dominant reaction during the electropolymerization of MB. All these peaks indicate that PMB polymer was successfully electropolymerized on ITO surface with this proposed method and was not homogeneous but still contain remaining MB traces, which was in accordance with those obtained by Hichem et al. [19].

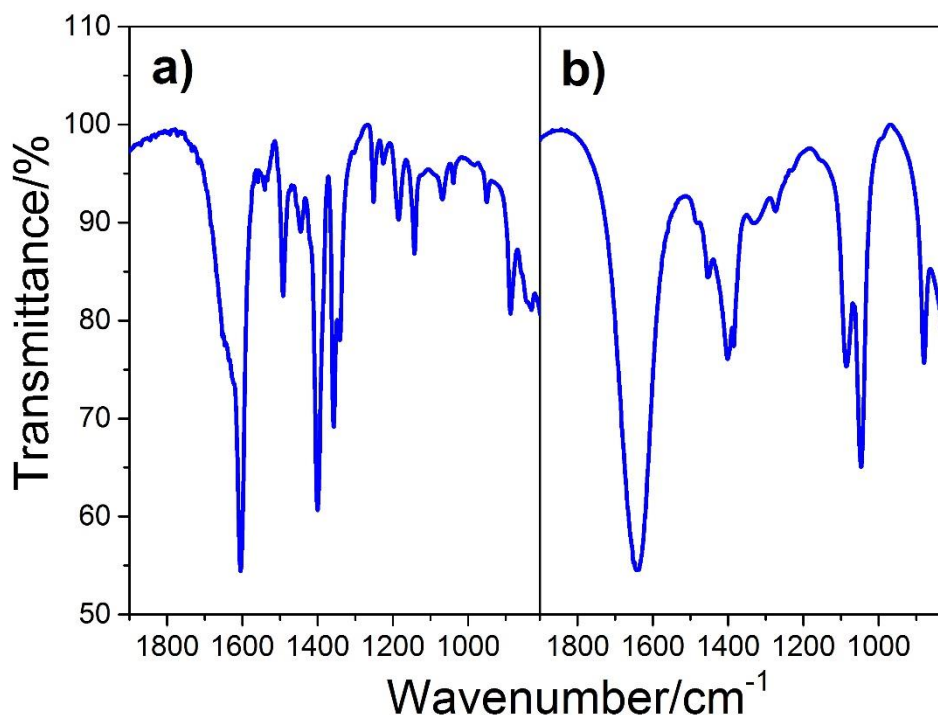


Figure 3. FTIR spectra of electropolymerized PMB (a) and MB monomer (b).

3.2. Growth and characterization of AuNPs

We demonstrated the electrochemical properties of the Au/PMB/ITO electrode by DPV in 0.5 M H_2SO_4 over the potential range from 0 to 1.3 V. After electro-oxidized at potential of +1.35 V for 120 s, the Au-PMB/ITO electrode gave a characteristic cathodic peak appearing at 0.93 V during a cathodic potential scan, which was attributed to the reduction of AuNPs oxide formed during an anodic potential sweep and in accordance with previous reports [21]. So we can confirmed that the AuNPs were formed on the PMB/ITO electrode surface.

To describe the morphology and size of the as-prepared gold nanoparticles, SEM was employed. The SEM measurements indicated that there was no obvious particles on the PMB/ITO substrate before immersed in the growth solution (growth time 0h). When the substrate was immersed in the growth solution, the positively charged MB monomer remaining in the PMB film could attract AuCl_4^- ions through the electrostatic attraction, reduce them to form AuNPs and serves as anchoring sites for AuNPs in situ growth. after treating the substrate in the growth solution for 1h, the presence

of AuNPs in a diameter of 40 ± 8 nm (Fig.5b, as determined by SEM) dispersed on the substrate surface was observed.

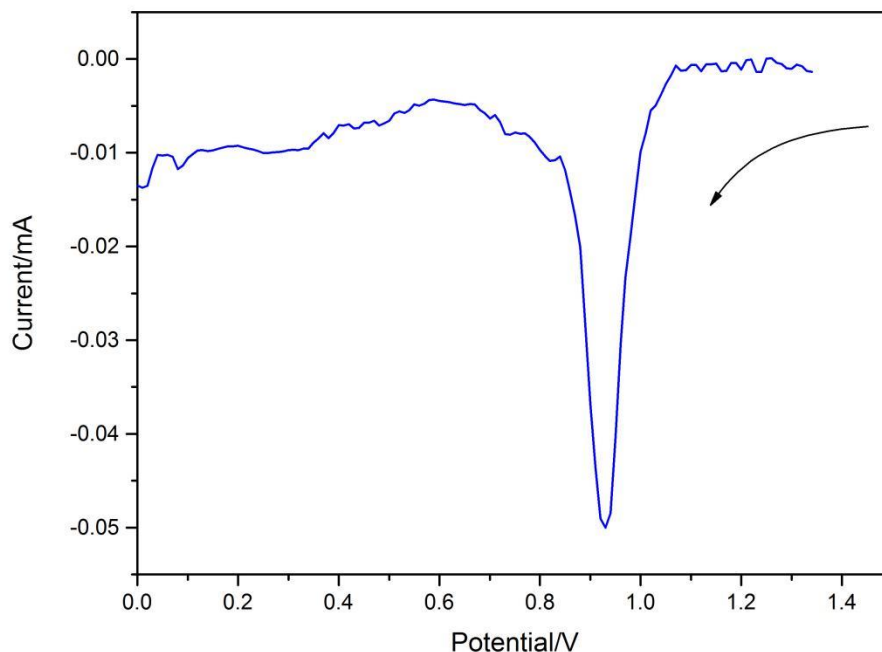


Figure 4. Characteristic reductive peak of gold oxide by DPV. Electrolyte: 0.5 M H_2SO_4 .

After the growth time with 4h, the size of the AuNPs was increased to 52 ± 8 nm (Fig. 5c). The particle size could be further increased to 99 ± 29 nm with growth time 8h, which was distributed uniformly on the substrate (Fig.5d). As can be seen from the results that very small AuNPs formed first and subsequently served as nucleation seeds for in situ growth of larger size AuNPs, which was in agreement with the seeding growth method [21].

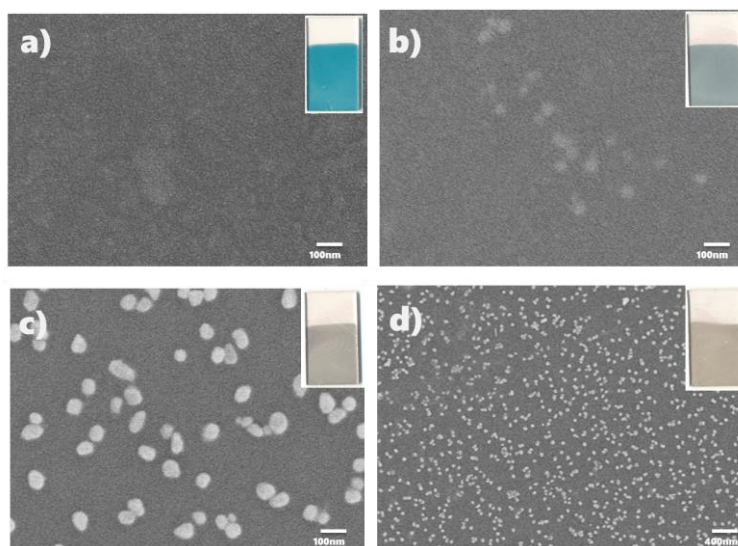


Figure 5. Time-dependent SEM images of AuNPs formed on the substrate with growth time: (a) 0h, (b) 1h, (c) 4h, and (d) 8h. The inset in the same figure shows the corresponding color of the substrate.

Meanwhile, the growth phenomenon (see the inset in the same figure) was also observable during the growth procedure. Before immersed in the growth solution, the substrate displays blue color, which is the color of PMB. After immersed in the growth solution for 1h, the substrate color becomes pearl blue due to the formation of small AuNPs. With increasing growth time, the color becomes dark yellow, while the growth solution turned transparent due to the reduction of AuCl_4^- ions by MB and the growth of AuNPs on the substrate. All phenomena above suggested the successful synthesis of AuNPs on the substrate by the proposed method.

3.3 Electrocatalytic properties of Au/PMB/ITO for glucose oxidation

To further investigate electrocatalytic activity of AuNPs, we examined the electrochemical response of glucose on Au/PMB/ITO, PMB/ITO and bare ITO electrode in 0.1 M NaOH containing 0.15 mM glucose. As can be seen in Fig.6a, several waves correlating with the electrooxidation of glucose were observed. The reaction started with a broad wave at around -0.1 V attributed to the adsorption of glucose on the Au/PMB/ITO surface. With further scan to more positive potential, the second wave appeared at around 0.34 V due to the oxidation of the adsorbed glucose intermediate to gluconolactone. In the backward scan, a sharp anodic peak appeared attributed to the re-oxidation of glucose, which is a two-electron process resulting in higher anodic current than in case of single electron reaction in the forward scan [22].

Meanwhile, compared with PMB/ITO and bare ITO electrode, no significant peak was observed during the scan, indicating they had no catalytic activity toward glucose oxidation.

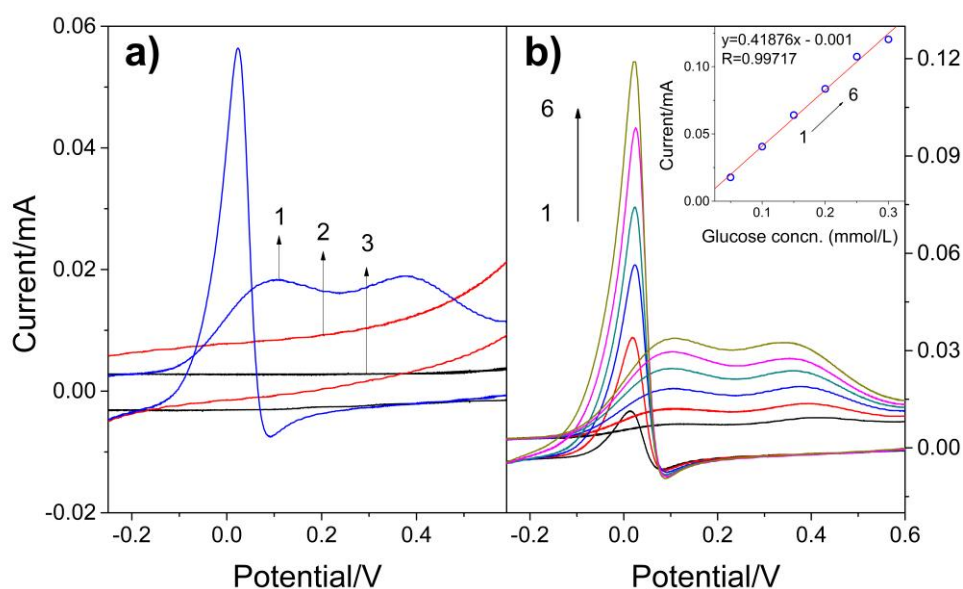


Figure 6. (a) CV of Au/PMB/ITO (1), PMB/ITO (2) and bare ITO (3) electrode in 0.1 M NaOH containing 1.5×10^{-4} M glucose. (b) the cyclic voltammetry response of Au/PMB/ITO in different concentrations of glucose (from 1 to 6: 5×10^{-5} , 1.0×10^{-4} , 1.5×10^{-4} , 2.0×10^{-4} , 2.5×10^{-4} , 3.0×10^{-4} M). Inset: the plot of peak current against the concentration of glucose. (vs. Ag/AgCl; scan rate: 100 mV/s)

The sensitivity of sensor was evaluated by CV of different concentrations of glucose in 0.1 M NaOH at scan rate of 100 mV s⁻¹. As shown in Fig. 6B, three peaks were observed attributed to the adsorption and the oxidation of glucose, respectively. Since the peak occurring in the backward scan displayed more distinguishable, the calibration curve was obtained by plotting the current value of this peak against the concentration of glucose. The resulting equation of linear regression was $y = 0.41876x - 0.001$ with the coefficient of determination $R^2 = 0.99717$ and the detection limit of 0.0097 mM (based on S/N = 3). The sensitivity calculated was 312 mA mM⁻¹cm⁻², which was 10-fold higher than that of previous study (Table 1) related to the detection of glucose on gold nanostructured surfaces [22 - 24].

Table 1. Comparison of electrochemical behavior of nanostructured gold sensors for non-enzymatic glucose detection.

Electrode	Applied potential (V)	Sensitivity (mA mM ⁻¹ cm ⁻²)	Detection limit (mM)	Ref.
Porous gold	+0.35	11.8	2 - 10	18
Porous gold cluster film	+0.10	10.8	0.01 - 10	19
Sawtooth-like gold	0.0	73.6	0.001 - 0.5	20
Au/PMB/ITO	-0.1	312	0.0097	This work

4. CONCLUSIONS

In this paper, we proposed a novel approach for in situ growth of highly-dispersed AuNPs on PMB/ITO electrode (Au/PMB/ITO) without using additional binding molecules and toxic reductants. MB monomer remaining in the PMB film served as not only the reductant to form AuNPs by reducing AuCl⁴⁺, but also as the anchor for AuNPs in situ growth to prevent the aggregation of AuNPs, thereby increasing their dispersity. The as-prepared AuNPs displayed an excellent electrocatalytic activity towards glucose oxidation with a higher sensitivity and a lower operating potential compared with other AuNPs modified electrodes and hold great promise in applications such as electroanalytical chemistry and biosensors.

ACKNOWLEDGMENTS

This work was supported by National Natural Science Foundation of China (21265005, 21565011), Guangxi Natural Science Foundation (2013GXNSFB053009, 2015GXNSFAA139020), the project of high level innovation team and outstanding scholar in Guangxi colleges and universities, Guangxi colleges and universities key laboratory of food safety and detection, collaborative innovation center for water pollution control and water safety in karst area, and the Guangxi key laboratory of environmental pollution control theory and technology.

References

1. V. Mani, B.V. Chikkaveeraiah, V. Patel, J.S. Gutkind and J.F. Rusling, *ACS Nano*, 3 (2009) 585.
2. M. Wei, L.G. Sun, Z.Y. Xie, J.F. Zhii, A. Fujishima, Y. Einaga, D.G. Fu, X.M. Wang and Z.Z. Gu, *Adv. Funct. Mater.*, 18 (2008) 1414.
3. X. Dai, G.G. Wildgoose, C. Salter, A. Crossley and R.G. Compton, *Anal. Chem.*, 78 (2006) 6102.
4. H. Pan, D. Li, J. Li, W. Zhu and L. Fang, *Int. J. Electrochem. Sci.*, 7 (2012) 12883.
5. Y. Ma, J. Di, X. Yan, M. Zhao, Z. Lu and Y. Tu, *Biosens. Bioelectron.*, 24 (2009) 1480.
6. H. Pan, S. Huang, X. Li, P. Li and W. Zhu, *Int. J. Electrochem. Sci.*, 11 (2016) 3364.
7. L.G. Abdelmohi and F.P. Zamborini, *Langmuir*, 26 (2010) 13511.
8. P.V. Dudin, P.R. Unwin and J.V. Macpherson, *Phys. Chem. Chem. Phys.*, 13 (2011) 17146.
9. H. Pan, D. Li, J. Liu, J. Li, W. Zhu and Y. Zhao, *J. Phys. Chem. C*, 115 (2011) 14461.
10. L. Chen, J. Li, C. Zhou, W. Zhu and H. Pan, *Optoelectron. Adv. Mater.–Rapid Commun.*, 8 (2014) 1200.
11. Y.Y. Fu, F.F. Liang, H.F. Tian and J.B. Hu, *Electrochim. Acta*, 120 (2014) 314.
12. N. Goluboff and R. Wheaton, *J. Pediatr.*, 58 (1961) 86.
13. R. Ziolkowski, M. Jarczewska, L. Gorski and E. Malinowska, *J. Electrochem. Soc.*, 160 (2013) B152.
14. J.C. Li, S.L. Mu and Y.F. Li, *Acta Phys. Chim. Sin.*, 17 (2001) 229.
15. A. Silber, N. Hampp and W. Schuhmann, *Biosens. Bioelectron.*, 11 (1996) 215.
16. I.H. Kaplan, K. Dagci and M. Alanyalioglu, *Electroanalysis*, 22 (2010) 2694.
17. J.C. Liu and S.L. Mu, *Synth. Met.*, 107 (1999) 159.
18. D.D. Schlereth, E. Katz and H.L. Schmidt, *Electroanalysis*, 7 (1995) 46.
19. H. Hichem, A. Djamila and A. Hania, *Electrochim. Acta*, 106 (2013) 69.
20. V. Kertesz, J. Bacsikai and G. Inzelt, *Electrochim. Acta*, 41 (1996) 2877.
21. J.D. Zhang, M. Kambayashi and M. Oyama, *Electroanalysis*, 17 (2005) 408.
22. T. Jurik, P. Podesva, Z. Farka, D. Kovar, P. Skladal and F. Foret, *Electrochim. Acta*, 188 (2016) 277.
23. L. Han, S. Zhang, L. Han, D.-P. Yang, C. Hou and A. Liu, *Electrochim. Acta*, 138 (2014) 109.
24. Y. Li, Y.-Y. Song, C. Yang and X.-H. Xia, *Electrochem. Commun.*, 9 (2007) 981.